

UHE NEUTRINO ASTRONOMY AND NEUTRINO OSCILLATIONS

V. Berezhinsky

*INFN, Laboratori Nazionali del Gran Sasso,
67010 Assergi (AQ) Italy*

ABSTRACT

UHE neutrinos with $E > 10^{17}$ eV can be produced by ultra-high energy cosmic rays (UHECR) interacting with CMB photons (*cosmogenic neutrinos*) and by top-down sources, such as topological defects (TD), superheavy dark matter (SHDM) and mirror matter. Cosmogenic neutrinos are reliably predicted and their fluxes can be numerically evaluated using the observed flux of UHECR. The lower limit for the flux is obtained for the case of pure proton composition of the observed UHECR. The rigorous upper limit for cosmogenic neutrino flux also exists. The maximum neutrino energy is determined by maximum energy of acceleration, which at least for the shock acceleration is expected not to exceed $10^{21} - 10^{22}$ eV. The top-down sources provide neutrino energies a few orders of magnitude higher, and this can be considered as a signature of these models. Oscillations play important role in UHE neutrino astronomy. At production of cosmogenic neutrinos τ -neutrinos are absent and $\bar{\nu}_e$ neutrinos are suppressed. These species, important for detection, appear in the observed fluxes due to oscillation. Mirror neutrinos cannot be observed directly, but due to oscillations to ordinary neutrinos they can provide the largest neutrino flux at the highest energies.

1. Introduction

The boundary $E_\nu \sim 10^{17}$ eV between HE and UHE neutrino astronomy is connected with observational technique. The neutrino observations with underwater/ice detectors are valid mostly for HE neutrino range. This is successful and well developed experimental technique. Two detectors, Baikal and AMANDA, has reached now the saturated statistics, two other arrays, IceCube and ANTARES, started the observations, and two projects, NESTOR and NEMO, are at the stage of testing.

The prospects for UHE neutrino astronomy appeared in 1960s soon after prediction of the GZK ¹⁾ cutoff. It has been realized ²⁾ that proton interaction with CMB photons at large redshifts in case of cosmological evolution of the sources can produce UHE neutrino fluxes much higher than the observed UHECR flux.

In 80s it was understood that topological defects can produce unstable superheavy particles with masses up to the GUT scale ³⁾ and neutrinos with tremendous energies can emerge due to this process ⁴⁾.

It has been proposed that UHE neutrinos can be detected observing the horizontal Extensive Air Showers (EAS) ⁵⁾. The exciting prospects for detection of UHE neutrinos have appeared with the ideas of space detection, e.g. in the projects EUSO⁶⁾ and OWL⁷⁾. At present there is well developed JEM-EUSO project ⁸⁾ with the prospects to start the observations in 2012 - 2013.

The basic idea of detection by EUSO is similar to the fluorescent technique for observations of extensive air showers (EAS) from the surface of the Earth. The UHE neutrino entering the Earth atmosphere produces an EAS. The known fraction of its energy, which reaches 90% , is radiated in form of isotropic fluorescent light. An optical telescope from the space detects it. Since the observatory is located at very large height (~ 400 km) in comparison with thickness of the atmosphere, the fraction of detected flux is known, and thus this is the calorimetric measurement (absorption of up-going photons is small). A telescope with diameter 2.5 m controls the area $\sim 10^5$ km² and has a threshold for EAS detection $E_{\text{th}} \sim 1 \times 10^{19}$ eV ⁸⁾.

The very efficient method of UHE neutrino detection is given by observations of radio emission by neutrino-induced showers in ice and lunar regolith. This method has been originally suggested by G. Askaryan in 60s ⁹⁾. Propagating in the matter the shower acquires excessive negative electric charge due to involvement of the matter electrons in knock-on process. The coherent Cerenkov radiation of these electrons produces the radio pulse. Recently this method has been confirmed by the laboratory measurements ¹⁰⁾. There were the experiments to search for such radiation from neutrino-induced showers in the Greenland and Antarctic ice and in the lunar regolith. In all cases the radio-emission can be observed only for neutrinos of extremely high energies. The upper limits on the flux of these neutrinos have been obtained: in GLUE experiment ¹¹⁾ by radiation from the moon, in FORTE experiment ¹²⁾ by radiation from the Greenland ice and in ANITA ¹³⁾ and RICE ¹⁴⁾ experiments from the Antarctic ice.

The characteristic feature of these detection methods is the high energy threshold $E \gtrsim 1 \times 10^{19} - 1 \times 10^{20}$ eV. How neutrinos of these energies can be produced?

The most conservative mechanism of UHE neutrino production is $p\gamma$ mechanism of collisions of accelerated protons/nuclei with low-energy CMB photons. To provide neutrinos with energies higher than 1×10^{20} eV the accelerated protons must have energies higher than 2×10^{21} eV. For non-relativistic shock acceleration this energy can reach optimistically 1×10^{21} eV. For relativistic shock this energy can be somewhat higher. To have neutrinos with higher energies one has to put his hopes on less developed ideas of acceleration such as acceleration in strong e-m waves, exotic plasma mechanisms of acceleration and unipolar induction.

The top-down scenarios can naturally provide neutrinos with energies higher and much higher than 1×10^{20} eV. The idea common for many mechanisms is given by existence of superheavy particles with very large masses up to GUT scale. In Grand Unified Theories (GUT) these particles (gauge bosons and higgses) are short-lived. In the cosmic space they are produced by Topological Defects (TD). The decay of these particles results in the parton cascade, which is terminated by production of pions and other hadrons. Neutrinos are produced in their decays.

The superheavy particles are naturally produced at post-inflationary stage of the universe. The most reliable mechanism of production is gravitational one. The masses

of the produced particles can reach $10^{13} - 10^{14}$ GeV. Protecting by some symmetry (e.g. gauge symmetry or discrete gauge symmetry like R-parity in supersymmetry), these particles can survive until present time and produce neutrinos in the decays or annihilation.

2. Effects of UHE neutrino oscillations

Characteristic distances to the sources of UHE neutrinos are much larger than maximum oscillation lengths. Taken as the maximum neutrino energy $E_{\max} \sim 10^{20}$ eV one obtains the maximum oscillation length of order of 100 pc

$$\ell_{\text{osc}}^{\max} = \frac{4\pi E_{\max}}{(\Delta m^2)_{\min}} \approx 120 \text{pc} \left(\frac{E}{10^{20} \text{eV}} \right) \left(\frac{7 \times 10^{-5} \text{eV}^2}{\Delta m^2} \right), \quad (1)$$

while the distances r to UHE neutrino sources even in our galaxy is of order of a few kpc. The relation $r \gg \ell_{\text{osc}}$ is often interpreted as a sufficient condition for flavour equipartition at observation $\nu_e : \nu_\mu : \nu_\tau = 1 : 1 : 1$. However, it is well known that this is not true for arbitrary flavour composition at generation. In the recent work ¹⁵⁾ the precise calculations for connection of the generation and observed flavour compositions are performed.

The basic idea of calculations in ¹⁵⁾ can be explained in the simplified form as follows.

Let us consider how observed flavour ratio is connected with flavour composition at generation in the limiting case $r \gg \ell_{\text{osc}}$. The flavour neutrino eigenstate ν_α is given by mixing of mass eigenstates ν_i as $\nu_\alpha = U_{\alpha k} \nu_k$, where $\alpha = e, \mu, \tau$, are flavour indicies, k are mass eigenstate indicies $k = 1, 2, 3$ and $U_{\alpha k}$ is the mixing matrix. In the most general case $U_{\alpha k}$ is expressed through solar θ_{12} and atmospheric θ_{23} neutrino mixing angles, and include also small U_{e3} term (see equation below). However with a good accuracy one may use $U_{e3} = 0$ and $\theta_{23} = \pi/4$ and thus obtain

$$U = \begin{pmatrix} c_{12} & s_{12} & U_{e3} \\ -s_{12}c_{23} & c_{12}c_{23} & s_{23} \\ s_{12}s_{23} & -c_{12}s_{23} & c_{23} \end{pmatrix} \rightarrow \begin{pmatrix} c_{12} & s_{12} & 0 \\ -\frac{s_{12}}{\sqrt{2}} & \frac{c_{12}}{\sqrt{2}} & \frac{1}{\sqrt{2}} \\ \frac{s_{12}}{\sqrt{2}} & -\frac{c_{12}}{\sqrt{2}} & \frac{1}{\sqrt{2}} \end{pmatrix}. \quad (2)$$

In the limiting case $r \gg \ell_{\text{osc}}$, $\langle \sin r/l_{\text{osc}} \rangle = 0$ and $\langle \sin^2 r/l_{\text{osc}} \rangle = \frac{1}{2}$, and the propagation matrix, which describes $\nu_\alpha \rightarrow \nu_\beta$ oscillation, is given by

$$P_{\alpha\beta} = \sum |U_{\alpha i}|^2 |U_{\beta i}|^2 \quad (3)$$

The propagation matrix $P_{\alpha\beta}$ given by Eq. (3) allows to calculate flavour composition at observation for given flavour composition at generation. In particular for normal generation composition valid for unsuppressed channels of π decays $\nu_e : \nu_\mu : \nu_\tau = 1 : 2 : 0$ one obtains from Eq. (3) the composition at observation 1:1:1.

In the work ¹⁵⁾ are given many examples of absence equipartition at observations: the suppression of muon decays in the chain of pion decay, production of neutrinos in neutron beam, decay of neutrinos and others.

3. Observational effects caused by oscillations

In this paper we will consider three observational effects caused by oscillations: (i) appearance of $\bar{\nu}_e$ neutrinos important for resonant reaction $\bar{\nu}_e + e^- \rightarrow W^- \rightarrow$ hadrons, (ii) appearance of τ neutrinos and oscillation of mirror to ordinary neutrinos. In this section we consider the first two effects; oscillations of mirror neutrinos will be discussed in section .

Resonant interaction of $\bar{\nu}_e$ neutrinos.

Glashow ¹⁶⁾ considered in 1960 the resonance reaction $\bar{\nu}_e + e^- \rightarrow W^- \rightarrow \mu^- + \bar{\nu}_\mu$. The resonance reaction $\bar{\nu}_e + e^- \rightarrow W^- \rightarrow$ hadrons was first suggested in 1977 in ¹⁷⁾. We will follow here the analytic approach of this paper.

The resonant production of W^- in $\bar{\nu}_e e$ collisions occurs at $\bar{\nu}_e$ energy

$$E_0 = \frac{m_W^2}{2m_e} = 6.3 \times 10^6 \text{GeV}. \quad (4)$$

Integrating over the Breit-Wigner resonance, one obtains analytically ¹⁷⁾ the rate of resonant events in underground detector with number of electrons N_e , given by

$$\nu_{\text{res}} = 2\pi\sigma_{\text{eff}}E_0J_{\bar{\nu}_e}(E_0)N_e, \quad (5)$$

where $J_{\bar{\nu}_e}(E_0)$ is the diffuse flux of UHE $\bar{\nu}_e$, 2π is the solid angle for which deep underground detector is open for UHE neutrino flux and σ_{eff} is the value left after integration over the Breit-Wigner formula, which has meaning of effective cross-section

$$\sigma_{\text{eff}} = \frac{8\pi}{3\sqrt{2}}G_F = 2.7 \times 10^{-32} \text{cm}^2, \quad (6)$$

where G_F is the Fermi constant.

For cosmogenic neutrinos produced in $p\gamma$ collisions with CMB photons, the production of $\bar{\nu}_e$ is strongly suppressed in comparison with ν_e neutrinos, because the latter are produced in the chain of decay of the positively charged pions: $\pi^+ \rightarrow \mu^+ \rightarrow \nu_e$, while $\bar{\nu}_e$ in the chain of decay of negatively charged pions $\pi^- \rightarrow \mu^- \rightarrow \bar{\nu}_e$. Production of π^+ occurs in the resonant reaction $p + \gamma \rightarrow \Delta^+$, while production of π^- goes through $p + \gamma \rightarrow p + \pi^- + \pi^-$ with a small cross-section. As has been first noted in ¹⁷⁾ $\bar{\nu}_\mu \rightarrow \nu_e$ oscillation considerably increases the flux of cosmogenic $\bar{\nu}_e$ neutrinos. If to take the generation flavour ratio $\bar{\nu}_e : \bar{\nu}_\mu : \bar{\nu}_\tau = 0:1:0$, we obtain from Eq. (3) the ratio at observation $\bar{\nu}_e : \bar{\nu}_\mu : \bar{\nu}_\tau = \frac{1}{2} : 1 : 1$. For this flavour ratio the resonant signal is seen well over the background.

Tau neutrinos

Tau neutrinos are not produced in the chain of pion decays and appear at observation due to oscillations.

In underground detectors tau-neutrinos produce the characteristic two-bang effect¹⁸⁾: the first hadronic shower appears in $\nu_\tau + N \rightarrow \tau + \text{hadrons}$ interaction, and the second one is produced by tau-lepton decay $\tau \rightarrow \nu_\tau + \text{hadrons}$. At energy of tau-neutrino $E \sim 10^{15}$ eV the distance between two showers is about 50 m, and such event can be observed in IceCube detector. The tau lepton propagating between two shower vertex radiates, like muon, the Cherenkov photons and this radiation can be also detected. Fig. 1 illustrates the detection of tau-neutrino in the deep-underground detector.

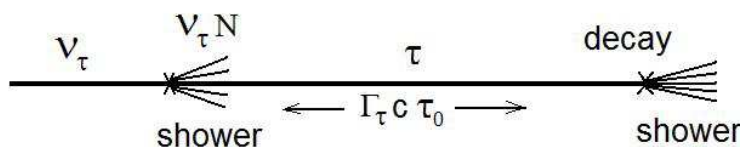


Figure 1: Double-bang effect produced by tau-neutrino in underground detector

The UHE neutrinos produce Earth-skimming effect¹⁹⁾, which can be observed by gigantic EAS arrays like the Auger detector. This is a mechanism of detection of

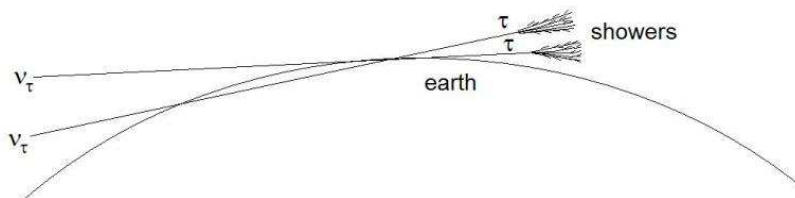


Figure 2: Earth-skimming effect produced by UHE tau-neutrinos, which can be observed by gigantic EAS detectors

horizontally moving neutrinos, but tau-neutrinos have the advantages in comparison with other neutrinos. Tau-neutrino can cross the large thickness of matter in the earth, due to effect of regeneration. Interacting with matter it produces tau-lepton, which at large energies propagates to large distance and decays producing again tau-neutrino. At energy $E \gtrsim 10^{18}$ eV tau-lepton has a decay length about 50 km and it can decay in the air producing hadrons which induce EAS propagating almost parallel to the Earth surface (see Fig. 2). The surface detectors register the EAS electromagnetic component from a lower part of EAS. In this way the upper limit on UHE tau-neutrinos was recently obtained at the Auger detector²⁰⁾.

4. Cosmogenic neutrinos in the dip model

Starting from pioneering work ²⁾ the fluxes of cosmogenic neutrinos have been calculated in many works ^{21) - 27)}. The predicted fluxes differ very considerably, depending on the different assumptions about mass composition of accelerated particles, on maximum energy of acceleration and on cosmological evolution of the sources. We shall present here the UHE neutrino fluxes calculated in the dip model for observed UHECR ^{28,29)}.

The dip model for UHECR

The pair production dip is a feature of interaction of extragalactic UHE protons propagating through CMB radiation. It is caused by energy losses of protons due to $p + \gamma_{\text{CMB}} \rightarrow e^+ + e^- + p$ scattering. This feature in proton spectrum, in principle, is very similar to the GZK cutoff which is caused by photopion production $p + \gamma_{\text{CMB}} \rightarrow N + \pi$. Both features are convenient to analyse in terms of *modification factor* $\eta(E)$, which is defined as a ratio of the diffuse proton spectrum $J_p(E)$ calculated with all energy losses included to the so-called unmodified spectrum $J_p^{\text{unm}}(E)$, when only adiabatic energy losses due to expansion of the universe are taken into account:

$$\eta(E) = \frac{J_p(E)}{J_p^{\text{unm}}(E)}, \quad (7)$$

The modification factor should be considered as the theoretical spectrum. Being defined as a ratio of two spectra it is free from many uncertainties. The modification factor is calculated using the power-law generation function $Q(E_g) \propto E_g^{-\gamma_g}$, where E_g is the energy of a proton at generation in a source and γ_g is the generation index. The calculated modification factor gives the excellent agreement with observational data for $\gamma_g = 2.6 - 2.7$ and for absence of source evolution, i.e. for evolutionary factor $(1+z)^m$ with $m = 0$. However, inclusion of evolution gives also good agreement with the data. This is not a surprising thing, since inclusion of evolution means introducing two additional free parameters, m and z_{max} . In Fig. 3 we show the comparison of the predicted dip and GZK cutoff with observational data of Akeno-AGASA, Yakutsk, HiRes and Auger detectors.

The observable part of the dip is extended from 1×10^{18} eV, where modification factor reaches 1, and up to 4×10^{19} eV, where the GZK cutoff begins. The agreement of the dip with all data is very good. However, one can see that the modification factor in the Akeno-AGASA data and in HiRes data exceeds 1 at $E \lesssim 1 \times 10^{18}$ eV. By definition the modification factor cannot be larger than 1. The excess of modification factor over 1 signals the appearance of the new component of cosmic rays, which can be nothing but galactic cosmic rays. Thus, this excess evidences for transition from galactic to extragalactic cosmic rays. Strictly speaking at the energy $E \sim 1 \times 10^{18}$ eV

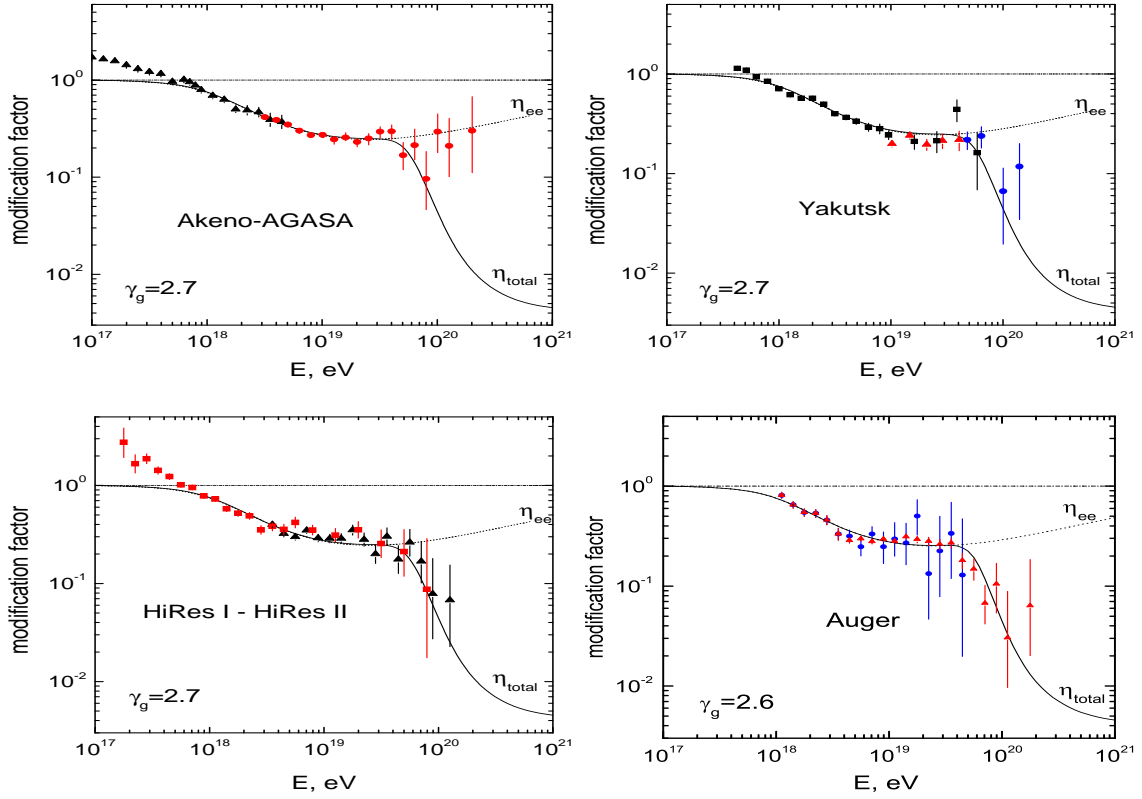


Figure 3: Theoretical pair-production dip and GZK cutoff in comparison with the observational data for non-evolutionary models with generation index $\gamma_g = 2.6 - 2.7$. The data of HiRes and Auger detectors show steepening of the spectrum consistent with the GZK cutoff. The excess of experimental modification factor over $\eta = 1$ at $E < 1 \times 10^{18}$ eV evidences for the new component, which is given by galactic cosmic rays.

transition is completed and at higher energy the cosmic rays are strongly dominated by extragalactic component. The transition occurs at lower energy, at the second knee seen at the range $(4 - 8) \times 10^{18}$ eV in the different experiments. The steepening observed in the HiRes spectrum is confirmed as the GZK feature by the measured value of $E_{1/2}$ in the integral spectrum. $E_{1/2}$ is a characteristic of the GZK cutoff in the integral spectrum³⁰⁾. It is defined as energy where the integral spectrum calculated with all energy losses included becomes half of the power-law extrapolation $KE^{-\gamma}$ from the low energies. In³⁰⁾ and²⁹⁾ it was demonstrated that $E_{1/2}$ is a model-independent value which equals to $10^{19.72}$ eV. Fig. 4 shows how $E_{1/2}$ was found from integral HiRes spectrum. The ratio $\kappa = J(> E)/KE^{-\gamma}$ is plotted as function of energy, where $J(> E)$ is measured integral spectrum and $KE^{-\gamma}$ is its power-law extrapolation. The equality $\kappa \approx 1$ shows that the chosen approximation is good. The energy where integral spectrum crosses the line $\kappa = 1/2$ gives $E_{1/2}$. The corresponding value is found³¹⁾ $E_{1/2} = 10^{19.73 \pm 0.07}$ in excellent agreement with the theoretical value.

The confirmation of the pair-production dip and the GZK cutoff in observational

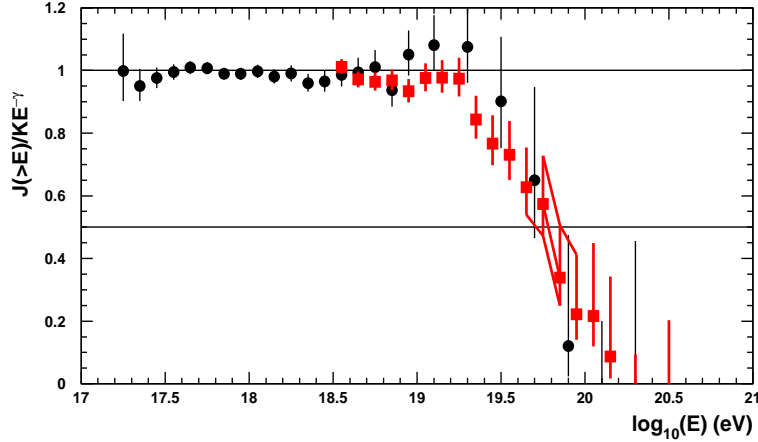


Figure 4: $E_{1/2}$ as numerical characteristic of the GZK cutoff in the integral HiRes spectrum.

data evidences that primary spectrum at $E \gtrsim 1 \times 10^{18}$ eV is strongly dominated by protons.

Neutrino fluxes in the dip model

To calculate the neutrino flux produced by UHE protons it is enough to know the generation rate of UHE protons at each cosmological epoch, which we take in the form $Q(E)(1+z)^m$, where factor $(1+z)^m$ describes the cosmological evolution of the sources. One should also introduce z_{\max} up to which the assumed evolution of the sources holds. $Q(E)$ gives the rate of proton generation at $z = 0$, i.e. the number of protons with energy E generated per unit of comoving volume per unit time. Expressed in terms of the Lorentz factor $\Gamma = E/m_p$ and the emissivity \mathcal{L}_0 at $z = 0$, i.e. energy generated per unit comoving volume and unit time, the generation rate is given by

$$Q(\Gamma) = (\gamma_g - 2) \frac{\mathcal{L}_0}{m_p} \Gamma^{-\gamma_g}, \quad (8)$$

where $\gamma_g = 2.6 - 2.7$ is the generation index and $\Gamma_{\min} \sim 1$ is assumed.

However, following the works ^{32,33)} we assume that acceleration index in each source is the same $\gamma_{\text{acc}} = 2.0 - 2.2$, but the maximum energies of acceleration E_{acc}^{\max} are different and distribution of sources over E_{acc}^{\max} results in steepening of the generation spectrum at $E \geq E_c$ to $\gamma_g \approx 2.6 - 2.7$.

The model with the *minimum UHE neutrino flux* corresponds to absence of the evolution $m = 0$ and low maximum energy of acceleration $E_{\text{acc}}^{\max} = 1 \times 10^{21}$ eV. Less important is the assumption for value of E_c , for which we use $E_c \sim 1 \times 10^{18}$ eV, The calculated minimum flux is shown in the upper panel of Fig. 5. This flux is very small, but it could be marginally detectable by IceCube at $E \gtrsim 10^{17}$ eV and by JEM-EUSO at $E \gtrsim 10^{19}$ eV.

One can maximize the flux introducing the cosmological evolution of the sources

and assuming high maximum acceleration energy. This flux is shown in the lower panel of Fig. 5 for the following choice of parameters: $m = 4.0$, $z_{\max} = 6.0$, $\gamma_g = 2.45$ and emissivity $\mathcal{L}_0 = 1.2 \times 10^{46}$ erg Mpc $^{-1}$ yr $^{-1}$. One may notice the worse agreement with the dip with than in the case of the non-evolutionary model.

Neutrino fluxes from AGN in the dip model

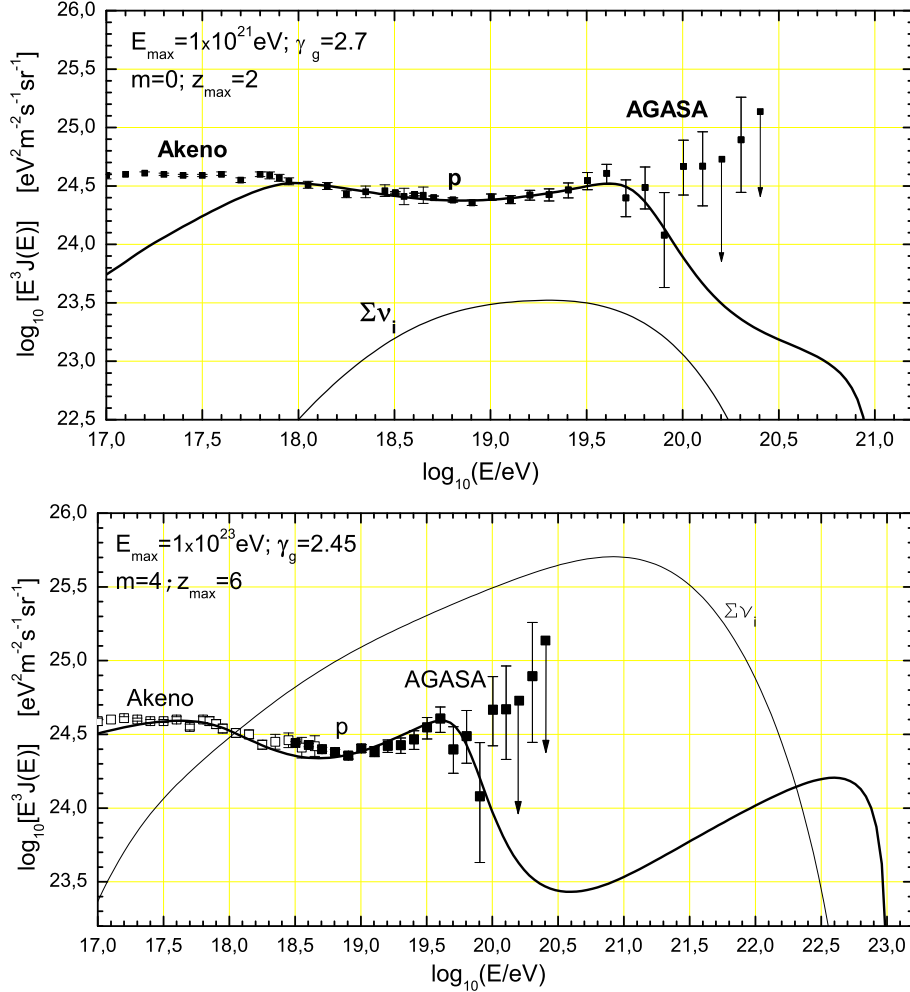


Figure 5: UHE neutrino fluxes in the non-evolutionary dip model (upper panel) and in the evolutionary dip model (lower panel). The neutrino fluxes are shown by curves $\Sigma \nu_i$ for the sum of all neutrino flavours. The following parameters are used in calculations: $m = 0$, $z_{\max} = 2$, $\gamma_g = 2.7$, $E_{\max} = 1 \times 10^{21}$ eV, $E_c = 1 \times 10^{18}$ eV and $\mathcal{L}_0 = 3.5 \times 10^{46}$ erg/Mpc 3 yr (upper panel). In the lower panel the neutrino flux is maximized by the following choice of parameters: $m = 4.0$, $z_{\max} = 6.0$, $\gamma_g = 2.45$ and emissivity $\mathcal{L}_0 = 1.2 \times 10^{46}$ erg Mpc $^{-1}$ yr $^{-1}$.

AGN are the most promising sources of the observed UHECR as far as acceleration and total energy output is concerned^{34,29)}. There are also some observational indications in the form of the correlations of UHECR particles with AGN^{35,36,37)}. We present here the results of calculations³⁸⁾ performed in phenomenological approach.

We assume the generation rate of UHE protons as described above with spectral index $\gamma_g = 2.0$ at $E \leq E_c$ and $\gamma_g = 2.52$ above this energy due to assumed distribution of AGN over E_{\max} . The value $\gamma_g = 2.52$ is chosen to provide the best fit to the dip (see Fig. 6). The UHE neutrino flux is calculated due to interaction with CMB. The evolution of AGN is taken according to X-ray observations³⁹⁾: $(1+z)^m$ with $m = 2.7$ up to $z_c = 1.2$. At larger z the evolution is frozen up to $z_{\max} = 2$. Notice, that this is very weak evolution, but even such evolution combined with $E_{\text{acc}}^{\max} = 1 \times 10^{22}$ eV makes UHE neutrino fluxes detectable by EUSO and radio detectors. Neutrino fluxes in Fig. 6 are given for one neutrino flavour.

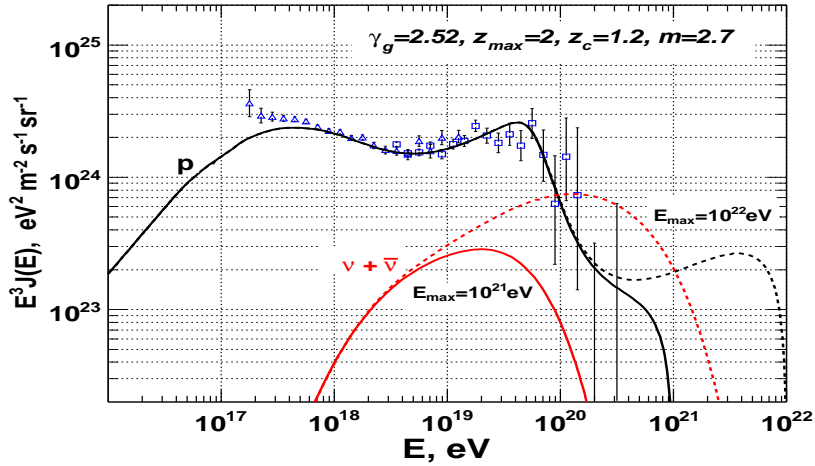


Figure 6: UHE neutrino flux in the dip model with AGN as the sources of UHECR. The cosmological evolution of AGN with $m = 2.7$ up to $z_c = 1.2$ is taken from X-ray observations of AGN. At larger z the evolution is frozen up to $z_{\max} = 2.0$. The fit of the dip is very good, though requires $\gamma_g = 2.52$ different from the non-evolutionary case $m = 0$. The neutrino fluxes are given for one neutrino flavour and they are detectable especially for the case $E_{\text{acc}}^{\max} = 1 \times 10^{22}$ eV.

5. Cascade upper limit on UHE neutrino flux

The Waxman-Bahcall⁴⁰⁾ upper bound is not applicable for UHE neutrinos. This bound is obtained from equality of the accompanying UHE proton flux and the observed flux of UHECR, assuming some relation between proton and neutrino fluxes at production. However, one can see from Fig. 5 that UHE neutrino fluxes differ for the same proton flux by two-three order of magnitudes at different energies (see upper and lower panels). The most interesting case of UHE neutrino flux produced by top-down models are not limited by the Waxman-Bahcall bound because accompanying proton flux is negligibly small and most produced particles are pions and kaons.

However, the Waxman-Bahcall limit is useful as a low-flux benchmark for the future experiments.

The most efficient upper bound for UHE neutrinos, applicable for both cosmogenic

neutrinos and neutrinos from top-down models, is given by the *cascade upper limit* first considered in ⁵⁾ (see also ⁴¹⁾).

The cascade upper limit on UHE neutrino fluxes ^{5,42,43)} is provided due to e-m cascades initiated by UHE photons or electrons which always accompany production of UHE neutrinos. Colliding with low-energy target photons, a primary photon or electron produce e-m cascade due to reactions $\gamma + \gamma_{\text{tar}} \rightarrow e^+ + e^-$, $e + \gamma_{\text{tar}} \rightarrow e' + \gamma'$, etc. (see Fig. 7). The standard case, valid for cosmogenic neutrinos, is given by production of UHE neutrinos in extragalactic space, and the cascade develops due to collisions with CMB photons ($\gamma_{\text{tar}} = \gamma_{\text{CMB}}$). In case neutrino production occurs in a galaxy, the accompanying photon can either freely escapes from a galaxy and produce cascade in extragalactic space, or produce cascade on the background radiation (e.g. on CMB or infrared) inside the galaxy. In the latter case the galaxy should be transparent for the cascade photons in the range 10 MeV - 100 GeV. The spectrum of the cascade

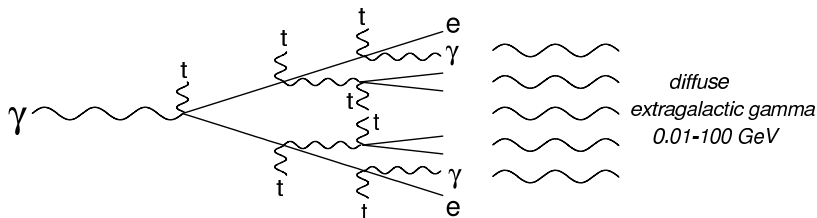


Figure 7: Electromagnetic cascade developing on the target photons (t), e.g. CMB.

photons is calculated ^{5,42,43,44)}: in low energy part it is $\propto E^{-3/2}$, at high energies $\propto E^{-2}$ with a cutoff at some energy ϵ_γ . The energy of transition between two regimes is given approximately by $\epsilon_c \approx (\epsilon_t/3)(\epsilon_\gamma/m_e)^2$, where ϵ_t is the mean energy of the target photon. In case the cascade develops in extragalactic space $\epsilon_t = 6.35 \times 10^{-4}$ eV, $\epsilon_\gamma \sim 100$ GeV (absorption on optical radiation), and $\epsilon_c \sim 8$ MeV. The cascade spectrum is very close to the EGRET observations in the range 3 MeV - 100 GeV ⁴⁵⁾. The observed energy density in this range is $\omega_{\text{EGRET}} \approx (2 - 3) \times 10^{-6}$ eV/cm³. It provides the upper limit for the cascade energy density. The upper limit on UHE neutrino flux $J_\nu(> E)$ (sum of all flavors) is given by chain of the following inequalities

$$\omega_{\text{cas}} > \frac{4\pi}{c} \int_E^\infty E J_\nu(E) dE > \frac{4\pi}{c} E \int_E^\infty J_\nu(E) dE \equiv \frac{4\pi}{c} E J_\nu(> E), \quad (9)$$

which in terms of the differential neutrino spectrum $J_\nu(E)$ gives

$$E^2 J_\nu(E) < \frac{c}{4\pi} \omega_{\text{cas}}, \quad \text{with } \omega_{\text{cas}} < \omega_{\text{EGRET}} \quad (10)$$

Eq. (10) gives the *rigorous* upper limit on the neutrino flux. It is valid for neutrinos produced by HE protons, by topological defects, by annihilation and decays

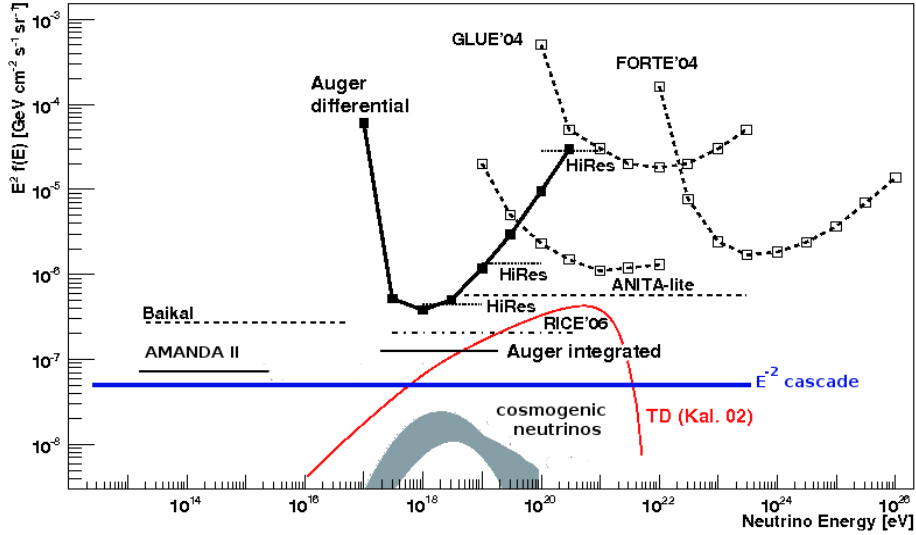


Figure 8: The experimental upper limits on UHE neutrino fluxes in comparison with the e-m cascade upper limit in assumption of E^{-2} generation spectrum (curve E^{-2} cascade) and with predictions for cosmogenic neutrinos and neutrinos from TDs ²²⁾. The plot is the modified one from ⁴⁶⁾.

of superheavy particles, i.e. in all cases when neutrinos are produced through decay of pions and kaons. It is valid for production of neutrinos in extragalactic space and in galaxies, if they are transparent for the cascade photons. It holds for arbitrary neutrino spectrum falling down with energy. If one assumes some specific shape of neutrino spectrum, the cascade limit becomes stronger. For E^{-2} generation spectrum, which is usually assumed for analysis of observational data one obtains the stronger upper limit. Given for one neutrino flavour it reads

$$E^2 J_i(E) \leq \frac{1}{3} \frac{c}{4\pi} \frac{\omega_{cas}}{\ln(E_{max}/E_{min})}, \quad (11)$$

where $i = \nu_\mu + \bar{\nu}_\mu$ or $i = \nu_e + \bar{\nu}_e$.

This upper limit is shown in Fig. 8. One can see that the observations almost reach the cascade upper limit and thus almost enter the region of allowed fluxes.

The most interesting energy range in Fig. 8 corresponds to $E_\nu > 10^{21}$ eV, where acceleration cannot provide protons with sufficient energy for production of these neutrinos. In fact this statement is valid only for shock acceleration. In principle, e.g. in AGN the different mechanisms of acceleration might operate, such as unipolar induction or pinch-instability, and they can provide the higher energy of acceleration, but these mechanisms are not developed enough for numerical calculations of produced fluxes of accelerated particles. At present the region of $E_\nu > 10^{21}$ eV, and especially $E_\nu \gg 10^{21}$ eV is considered as a signature of top-down models, which provide these energies quite naturally. Below we shall consider three top-down models: Superheavy

6. UHE neutrinos from Superheavy Dark Matter (SHDM)

SHDM is one of the models for cosmological cold dark matter ^{47,48}). The most attractive mechanism of production is given by creation of superheavy particles in time-varying gravitational field in post-inflation epoch ^{49,50}). Creation occurs when the Hubble parameter is of order of particle mass $H(t) \sim m_X$. Since the maximum value of the Hubble parameter is limited by the mass of the inflaton $H(t) \lesssim m_\phi \sim 10^{13}$ GeV, the mass of X-particle is limited by m_ϕ , too. For example, $m_X \sim 3 \times 10^{13}$ GeV results in $\Omega_X h^2 \sim 0.1$, as required by WMAP measurements.

Being protected by some symmetry, SHDM particles with such masses can be stable or quasi-stable. In case of gauge symmetry they are stable, in case of gauge discrete symmetry they can be stable or quasi-stable. Decay can be provided by superweak effects: wormholes, instantons, high-dimension operators etc.

Like any other form of cold dark matter, X-particles are accumulated in the halo with overdensity 2.1×10^5 .

SHDM particles can produce UHECR and high energy neutrinos at the decay of X-particles (when the protecting symmetry is broken) and at their annihilation, when the symmetry is exact. The scenario with decaying X-particles was first studied in ^{47,51,52}). An interesting scenario with stable X-particles, when UHE particles are produced by annihilation of X-particles has been put forward in ⁵³). In this scenario superheavy X-particles have the gauge charge and they are produced at post-inflationary epoch by close pairs, forming the bound systems. Loosing the angular momentum, these particles inevitably annihilate in a close pair.

The UHE particles (protons, pions and neutrinos from the chain of pion decays) are produced as a result of QCD cascading of partons. The calculations of fluxes and spectra are nowadays reliably performed by Monte Carlo ⁵⁴) and using the DGLAP equations ⁵⁵) - ⁵⁷). The spectra of protons, photons and neutrinos are shown in Fig. 9 for the case of SHDM particles with mass $M_X = 1 \times 10^{14}$ GeV. The spectrum of photons is normalized by the AGASA excess. In case it is absent, like in HiRes and Auger observations, all fluxes, including neutrino, must be lowered by factor 3 - 5.

7. UHE neutrinos from Topological Defects (TDs)

As has been first noticed by D. A. Kirzhnits ⁵⁸), each spontaneous symmetry breaking in the early universe is accompanied by the phase transition. Like the phase transitions in liquids and solids, the cosmological phase transitions can give rise to topological defects (TDs), which can be in the form of surfaces (cosmic textures), lines (cosmic strings) and points (monopoles). In many cases TDs become unstable and

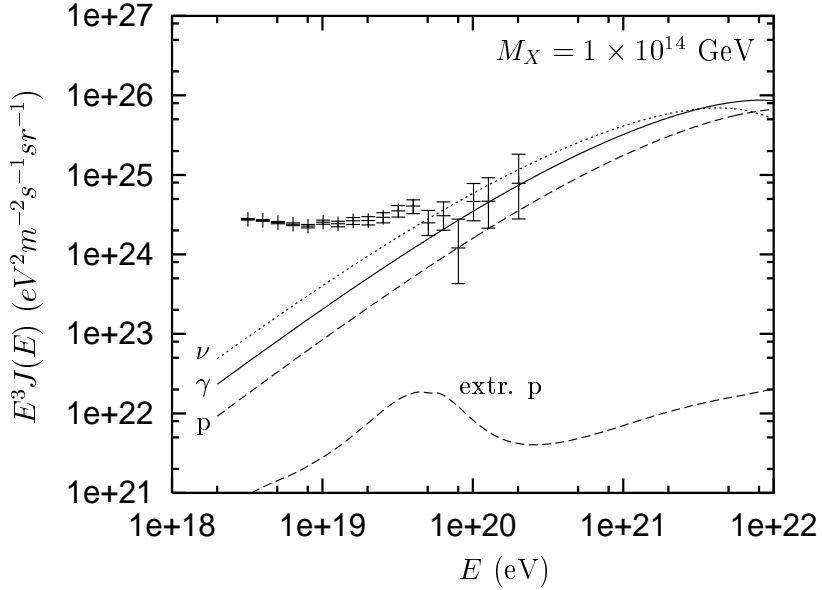


Figure 9: Spectra of neutrinos (upper curve), photons (middle curve) and protons (two lower curves) in SHDM model compared with AGASA data, according to calculations of ⁵⁷⁾. The neutrino flux is dominated by the halo component with small admixture of extragalactic flux. The flux of extragalactic protons is shown by the lower curve (extr. p). The fluxes are normalized by the AGASA excess at $E \gtrsim 1 \times 10^{20}$ eV. In case it is absent, like in HiRes and Auger data, all fluxes, including neutrino, must be lowered by factor 3 - 5.

decompose to constituent fields, superheavy gauge and Higgs bosons (X-particles), which then decay producing UHECR. It could happen, for example, when two segments of ordinary string, or monopole and antimonopole touch each other, when electrical current in superconducting string reaches the critical value and in some other cases. The decays of these particles, if they heavy enough, produce particles of ultrahigh energies including neutrinos.

The following TDs are of interest for UHECR and neutrinos ⁵⁹⁾: *monopoles* ($G \rightarrow H \times U(1)$ symmetry breaking), *ordinary strings* ($U(1)$ symmetry breaking) with important subclass of superconducting strings, *monopoles connected by strings* ($G \rightarrow H \times U(1)$ symmetry breaking with subsequent $U(1) \rightarrow Z_N$ symmetry breaking, where Z_N is discrete symmetry). The important subclass of the monopole-string network is given by *necklaces*, when $Z_N = Z_2$, i.e. each monopole is attached to two strings. We shall shortly describe the production of UHE particles by these TDs. (see ⁵⁹⁾ for more details).

(i) *Ordinary strings.*

There are several mechanisms by which ordinary strings can produce UHE particles. For a special choice of initial conditions, an ordinary string loop can collapse to a double line, releasing its total energy in the form of X-particles. However, the probability of this mode of collapse is extremely small, and its contribution to the

overall flux of UHE particles is negligible.

String loops can also produce X-particles when they self-intersect. Each intersection, however, gives only a few particles, and the corresponding flux is very small.

The loops undergo oscillation and an important property of it is the periodic appearance of the cusps, the loop points with velocity of light. The near-cusp segments, moving with large Lorentz factor may overlap and annihilate producing the constituent superheavy particles with large Lorentz factors. Therefore the particles from X-decays are further boosted by large Lorentz factor. The energy released in a single cusp event can be quite large, but again, the resulting flux of UHE particles is too small to account for the UHECR observations.

(ii) *Superconducting strings.*

As was first noted by Witten³⁾, in a wide class of elementary particle models, strings behave like superconducting wires. Moving through cosmic magnetic fields, such strings develop electric currents. Superconducting strings produce X-particles when the electric current in the strings reaches the critical value. This process is strongly increased in cusps where in a small fraction of loop the current becomes supercritical and X-particles, the charge carriers, leave the string and are decaying to the high-energy ordinary particles. Their energies are further boosted by cusp Lorentz factor. Superconducting strings cannot be the sources of observed UHECR⁵⁹⁾ because of the absorption of the particles on the way from a source to observer, but they can produce the observable flux of UHE neutrinos.

(iii) *Network of monopoles connected by strings.*

The sequence of phase transitions

$$G \rightarrow H \times U(1) \rightarrow H \times Z_N \quad (12)$$

results in the formation of monopole-string networks in which each monopole is attached to N strings. Most of the monopoles and most of the strings belong to one infinite network. The evolution of networks is expected to be scale-invariant with a characteristic distance between monopoles $d = \kappa t$, where t is the age of Universe and $\kappa = const$. The production of UHE particles are considered in⁶⁰⁾. Each string attached to a monopole pulls it with a force equal to the string tension, $\mu \sim \eta_s^2$, where η_s is the symmetry breaking vev of strings. Then monopoles have a typical acceleration $a \sim \mu/m$, energy $E \sim \mu d$ and Lorentz factor $\Gamma_m \sim \mu d/m$, where m is the mass of the monopole. Monopole moving with acceleration can, in principle, radiate gauge quanta, such as photons, gluons and weak gauge bosons, if the mass of gauge quantum (or the virtuality Q^2 in the case of gluon) is smaller than the monopole acceleration. The typical energy of radiated quanta in this case is $\epsilon \sim \Gamma_m a$. This energy can be much higher than what is observed in UHECR. However, the produced flux (see⁵⁹⁾) is much smaller than the observed one.

(vi) *Necklaces.*

Necklaces are hybrid TDs corresponding to the case $N = 2$, i.e. to the case when

each monopole is attached to two strings. This system resembles “ordinary” cosmic strings, except the strings look like necklaces with monopoles playing the role of beads. The evolution of necklaces depends strongly on the parameter

$$r = m/\mu d, \quad (13)$$

where m is a mass of a monopole, μ is mass per unit length of a string (tension of a string) and d is the average separation between monopoles and antimonopoles along the strings. As it is argued in Ref. ⁶¹⁾, necklaces might evolve to configurations with $r \gg 1$. Monopoles and antimonopoles trapped in the necklaces inevitably annihilate in the end, producing first the heavy Higgs and gauge bosons (X -particles) and then hadrons. The rate of X -particle production can be estimated as ⁶¹⁾

$$\dot{n}_X \sim \frac{r^2 \mu}{t^3 m_X}. \quad (14)$$

This rate determines the rates of pion and neutrino production with energy spectrum calculated in Ref. ⁵⁷⁾. Restriction due to e-m cascade radiation demands the cascade

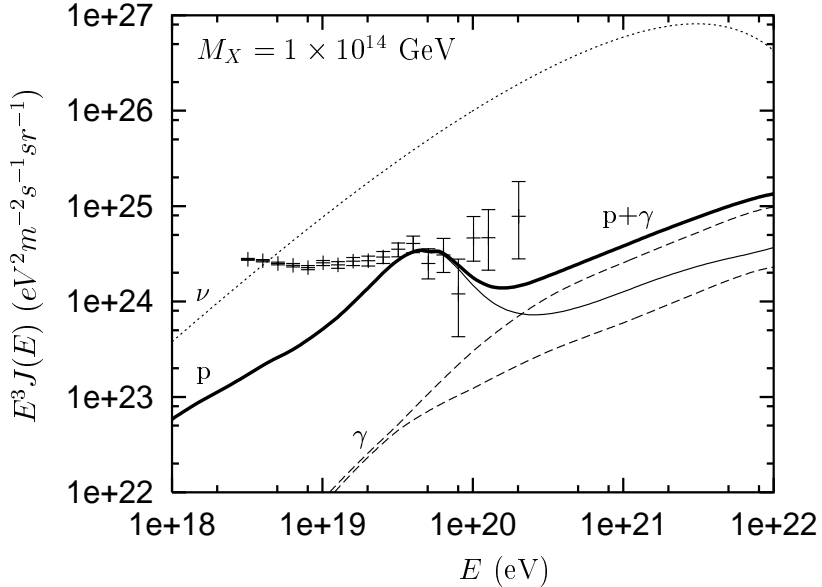


Figure 10: Diffuse spectra of neutrinos, protons and photons from necklaces. The upper curve shows neutrino flux, the middle - proton flux and two lower curves - photon fluxes for two cases of absorption. The thick curve gives the sum of the proton and the higher photon flux.

energy density $\omega_{cas} \leq 2 \cdot 10^{-6} \text{ eV/cm}^3$. The cascade energy density produced by necklaces can be calculated as

$$\omega_{cas} = \frac{1}{2} f_\pi r^2 \mu \int_0^{t_0} \frac{dt}{t^3} \frac{1}{(1+z)^4} = \frac{3}{4} f_\pi r^2 \frac{\mu}{t_0^2}, \quad (15)$$

where $f_\pi \approx 0.5$ is a fraction of total energy release transferred to the cascade. Therefore, $r^2\mu$ and the rate of X-particle production (14) is limited by cascade radiation.

The fluxes of UHE protons, photons and neutrinos from necklaces are shown in Fig. 10 according to calculations of ⁵⁷⁾. The mass of X-particle is taken $m_X = 1 \times 10^{14}$ GeV. Neutrino flux is noticeably higher than in the case of conservative scenarios for cosmogenic neutrinos and neutrinos from SHDM.

In the recent work ⁶²⁾ it was indicated that in some models of necklaces there could be fast annihilation of monopoles and separation of pairs monopole-antimonopole connected by strings from the necklaces. In these models UHE neutrino flux is suppressed. However, in some other models the detectable neutrino flux can exist.

8. Mirror matter and mirror neutrinos

Existence of mirror matter in our universe is the old idea which was put forward in the end of 1950s. Mirror matter can be most powerful source of UHE neutrinos not limited by e-m cascade limit. Produced as the mirror neutrinos, they can oscillate into ordinary neutrinos. All mirror particles that accompany production of mirror neutrinos in the mirror matter remain invisible for our detectors.

Concept of mirror matter

Mirror matter is based on the theoretical concept of the space reflection, as first suggested by Lee and Yang ⁶³⁾ in 1956 and developed by Landau ⁶⁴⁾ in 1957, Salam ⁶⁵⁾ in 1957, and most notably by Kobzarev, Okun, Pomeranchuk ⁶⁶⁾ in 1966 (see recent exciting historical review by Okun ⁶⁷⁾).

This concept can be explained in the following way.

The Hilbert particle space is assumed to be a representation of the extended Lorentz group, which includes the space coordinate reflection $\vec{x} \rightarrow -\vec{x}$. Since the coordinate operations, reflection $\vec{x} \rightarrow -\vec{x}$ and time shift $t \rightarrow t + \Delta t$, commute, the corresponding operations in the particle space, I_r and Hamiltonian H , must commute, too:

$$[\mathcal{H}, I_r] = 0 \quad (16)$$

It implies that operator I_r must correspond to the conserved value. Since parity P according to assumption of Lee and Yang is not conserved, I_r should be defined somehow else. Lee and Yang suggested $I_r = P \times R$, where R transfers particle to mirror particle. Since parity operator P interchange left and right states, one obtains

$$I_r \Psi_L = \Psi'_R \quad \text{and} \quad I_r \Psi_R = \Psi'_L, \quad (17)$$

where primes indicate the states in mirror particle space.

The assumption of Landau ⁶⁴⁾ was $R = C$, i.e. one may say that he suggested to use antiparticles as the mirror space, but then CP must be conserved which as we

know today is not the case.

Oscillation of mirror and ordinary neutrinos

Kobzarev, Okun, and Pomeranchuk,⁶⁶⁾ suggested that ordinary and mirror sectors communicate only gravitationally. For the description of this interaction one can use dimension 5 operator obtained as $SU(2)_L \times U(1) \times SU(2)'_R \times U(1)'$ scalar:

$$\mathcal{L}_{\text{comm}} = \frac{1}{M_{\text{Pl}}} (\nu_L \phi) (\nu'_R \phi'), \quad (18)$$

where $M_{\text{Pl}} = 1.2 \times 10^{19}$ GeV is the Planckian mass, which implies the gravitational interaction, and ϕ, ϕ' are the electroweak Higgses from visible and mirror sectors,

After spontaneous electroweak symmetry breaking $\langle \phi \rangle = \langle \phi' \rangle = v$ the Lagrangian (18) generates the terms, which mix visible and sterile neutrinos,

$$\mathcal{L}_{\text{mix}} = \frac{v^2}{M_{\text{Pl}}} \nu \nu', \quad (19)$$

where $v = 174$ GeV is vacuum expectation value of Higgses, and $\mu = v^2/M_{\text{Pl}} = 2.5 \times 10^{-6}$ eV is the mixing parameter.

Eq. (19) implies oscillation of mirror and ordinary neutrinos. This oscillation described by Eq. (19), but with M not necessarily being the Planckian mass, was first suggested by Berezhiani and Mohapatra⁶⁸⁾ and Foot and Volkas⁶⁹⁾ in 1995.

UHE neutrinos from mirror TDs

Any cosmological scenario for mixed ordinary and mirror matter must provide the suppression of the mirror matter and in particular the density of mirror photons and neutrinos at the epoch of nucleosynthesis. It can be obtained in the two-inflaton model⁷⁰⁾. The rolling of two inflatons to minimum of the potential is not synchronized, and when the mirror inflaton reaches minimum, the ordinary inflaton continues its rolling, inflating thus the mirror matter produced by the mirror inflaton. While mirror matter density is suppressed, the mirror topological defects in two-inflatons scenario with curvature-driven phase transition can strongly dominate⁷⁰⁾. Mirror TDs copiously produce mirror neutrinos with extremely high energies typical for TDs, and they are not accompanied by any visible particles. Therefore, the upper limits on HE mirror neutrinos in our world do not exist. All HE mirror particles produced by mirror TDs are sterile for us, interacting with ordinary matter only gravitationally, and only mirror neutrinos can be efficiently converted into ordinary ones due to oscillations. The oscillations of mirror and visible neutrinos in the gravitational-mixing scenario has been studied in detail in⁷¹⁾. The probability of oscillation of mirror neutrino ν' into visible neutrinos is large. In particular, for ν'_μ neutrino it is given by

$$P_{\nu'_\mu \nu_e} = \frac{1}{8} \sin^2 2\theta_{12}, \quad P_{\nu'_\mu \nu_\mu} = P_{\nu'_\mu \nu_\tau} = \frac{1}{4} - \frac{1}{6} \sin^2 2\theta_{12}, \quad \sum_\alpha P_{\nu'_\mu \nu_\alpha} = \frac{1}{2}. \quad (20)$$

9. Conclusions

UHE neutrino astronomy is characterised by well balanced program.

As the secure part of this program, there are cosmogenic neutrinos, for production of which the particle beam (UHECR particles) and the target (CMB photons) are well known. In the case when UHECR primaries are protons and the observed dip is a feature of UHE proton interaction with CMB, there is the robustly predicted *lower limit* for UHE neutrino flux (see upper panel of Fig. 5), which is marginally detectable by IceCube at $E < 1 \times 10^{18}$ eV and by JEM-EUSO at $E > 1 \times 10^{19}$ eV. This lower limit is supported by the following observations: the features of UHE proton interaction with CMB, GZK cutoff and dip, are found, mostly in HiRes observations, and the fluorescent data of HiRes evidence for proton-dominated mass composition. However, the Auger fluorescent data favour the mixed nuclei composition. In this case the cosmogenic neutrinos can be undetectable for existing projects.

The large fluxes of cosmogenic neutrinos, detectable by existing projects, correspond (at the fixed UHECR flux) to cosmological evolution of the sources, flat generation spectra and large maximum energy of acceleration. The lower panel of Fig. 5 presents UHE neutrino fluxes for the extreme hypothetical assumptions: very large E_{\max} and strong evolution of the sources up to $z_{\max} = 6$.

The fundamental problem of astrophysics involved in prediction of UHE cosmogenic neutrinos is acceleration of particles. The shock acceleration at present knowledge of its theory cannot provide maximum energy of acceleration higher than $10^{21} - 10^{22}$ eV, and thus energies of cosmogenic neutrinos do not exceed 3×10^{20} eV. However, in case of AGN as UHECR sources, the alternative mechanisms of acceleration, such as unipolar induction and plasma mechanisms, can work and accelerate particles to much higher energies. Unfortunately, these mechanisms are not developed enough for numerical calculations of produced rates and spectra at generation. The detection of UHE neutrinos from the individual sources can help to solve this fundamental problem of astrophysics.

The second part of UHE neutrino astronomy is provided by top-down sources: SHDM and topological defects in ordinary and mirror matter. The decays of unstable constituent fields of TDs can produce neutrinos with extremely high energies up to GUT scale and above. This is the general property of top-down models. However, the fluxes are very model dependent, and in case of TDs they differ much for different types of topological defects. There could be no flux estimates based on the general common properties of all TDs: some of them give low undetectable fluxes, from some exceptional TDs one can expect the detectable fluxes. For long time the necklaces have been considered as most promising TDs for UHECR and neutrinos⁶¹⁾, but recent work⁶²⁾ puts the doubts on these topological defects as sources of UHE particles in recent cosmological epochs. The signature of top-down models is very high neutrino

energies, unreachable for accelerator neutrinos. These neutrinos are most reliably detectable by radio and acoustic methods, as well as by EUSO detectors.

In both cases of cosmogenic and top-down models, the neutrino fluxes are constrained by the cascade upper limit. As exception, the mirror neutrinos do not respect this limit, and their fluxes can be even larger.

The search for UHE neutrinos in any case is a search for a new physics, either for astrophysics (the new acceleration mechanisms and cosmological evolution of the sources) or for topological defects, mirror topological defects and superheavy dark matter.

10. Acknowledgments

I am grateful to my collaborators Roberto Aloisio, Pasquale Blasi, Askhat Gazizov, Svetlana Grigorieva, Alex Vilenkin and Francesco Vissani for joint work and many useful discussions. This work is partially supported by contract ASI-INAF I/088/06/0 for theoretical studies in High Energy Astrophysics.

11. References

- 1) K. Greisen, Phys. Rev. Lett. **16**, 748 (1966), G. T. Zatsepin and V. A. Kuzmin, Pisma Zh. Experm. Theor. Phys. **4**, 114 (1966).
- 2) V. S. Berezinsky and G. T. Zatsepin, Phys. Lett **B 28**, 423 (1969); V. S. Berezinsky and G. T. Zatsepin, Soviet Journal of Nuclear Physics **11**, 111 (1970).
- 3) E. Witten, Nucl. Phys. B **249**, 557 (1985).
- 4) C. T. Hill, D. N. Schramm and T. P. Walker, Phys. Rev. D **36**, 1007 (1987).
- 5) V. Berezinsky and A. Smirnov, Ap. Sp. Sci., **32**, 461 (1975).
- 6) see <http://www.euso-misson.org/>
- 7) see <http://heawww.gsfc.nasa.gov/docs/gamcosray/hecr/OWL/>.
- 8) see <http://www.jemeuso.riken.jp/>
- 9) G. Askarian, JETP, **14** (1962) and **21** (1965).
- 10) D. Saltzberg, Phys. Rev. Lett. **86**, 2802 (2001); P. W. Gorham et al, hep-ex/0611008.
- 11) P. W. Gorham et al, Phys. Rev. Lett. **93**, 041101 (2004)
- 12) N. Lehtinen et al, Phys. Rev. D **69**, 013008 (2004)
- 13) S. W. Barwick et al., Phys. Rev. Lett. **96**, 171101 (2006)
- 14) I. Kravchenko et al, Astrop. Phys., **19**, 15 (2003).
- 15) S. Pakvasa, W. Rodejohann, T. Weiler, hep-ph/0711.4517
- 16) S. L. Glashow, Phys. Rev. **118**, 316 (1960).
- 17) V. S. Berezinsky and A. Z. Gazizov, JETP Lett. **25**, 254 (1977).
- 18) J. Learned, S. Pakvasa, Astropart.Phys. **3**, **267** (1995).

- 19) D. Fargion, *Astrophys.J.* **570**, 909 (2002), arXiv:astro-ph/0002453.
- 20) J. Abraham et al (Auger Collaboration), arXiv:0712.1909.
- 21) R. Engel, D. Seckel and T. Stanev, *Phys. Rev. D* **64**, 093010 (2001).
- 22) O. E. Kalashev, V. A. Kuzmin, D. V. Semikoz and G. Sigl, *Phys. Rev. D* **66**, 063004 (2002).
- 23) Z. Fodor, S. Katz, A. Ringwald and H. Tu, *JCAP* **0311**, 015 (2003).
- 24) D. Hooper, A. Taylor, S. Sarkar, *Astropart.Phys.* **23**, 11 (2005).
- 25) Maximo Ave et al., *Astropart.Phys.* **23**, 19 (2005).
- 26) D. Seckel, T. Stanev, astro-ph/0502244.
- 27) D. Allard et al., *JCAP* 0609, 005 (2006).
- 28) V. Berezhinsky, A. Z. Gazizov and S. I. Grigorieva, *Phys. Lett. B* **612**, 147 (2005).
- 29) V. Berezhinsky, A. Z. Gazizov and S. I. Grigorieva, *Phys. Rev. D* **74**, 043005 (2006); hep-ph/0204357.
- 30) V. Berezhinsky, and S. I. Grigorieva, *Astron.Astrophys.* **199**,1 (1988).
- 31) HiRes Collaboration, *Phys. Rev. Lett.* **100**, 101101 (2008); arXiv:astro-ph/0703099 v1.
- 32) M. Kachelriess, D. V. Semikoz, *Phys.Lett. B* **634**, 143 (2006).
- 33) R. Aloisio et al, *Astropart.Phys.* **27**, 76 (2007).
- 34) V. Berezhinsky, A. Z. Gazizov and S. I. Grigorieva, astro-ph/0210095.
- 35) P. G. Tinyakov and I. I. Tkachev, *JETP Lett.*, **74**, 445 (2001).
- 36) R. Jansson, G. R. Farrar, *JCAP* **06**, 017 (2008).
- 37) Pierre Auger Collaboration, *Astroparticle Physics* **29**, 188 (2008).
- 38) V. Berezhinsky, A. Gazizov, S. Grigorieva, in: astro-ph/0509675.
- 39) Y. Ueda et al, *Astrophys. J.*, **598**, 886 (2003);
A. J. Barger et al, *Astron. J.* **129**, 578 (2005).
- 40) E. Waxman and J. Bahcall, *Phys. Rev. D* **59**, 023002 (1999).
- 41) V. Berezhinsky, *Nucl. Phys. B (Proc. Suppl.)* **151**, 260 (2006); arXiv:astro-ph/0505220.
- 42) V. S. Berezhinsky, S. V. Bulanov, V. A. Dogiel, V. L. Ginzburg and V. S. Ptuskin, *Astrophysics of Cosmic Rays*, North-Holland 1990.
- 43) V. Berezhinsky, *Nucl. Phys. B* **380**, 478 (1992);
- 44) C. Ferrigno, P. Blasi, D. De Marco, astro-ph/0404352.
- 45) P. Sreekumar et al. [EGRET collaboration], *Astroph. J.* **494**, 523 (1998).
- 46) K. H. Kampert, arXiv:0801.1986.
- 47) V. Berezhinsky, M. Kachelriess, A. Vilenkin, *Phys. Rev. Lett.* **79**, 4302 (1997).
- 48) E. W. Kolb, D. J. H. Chung, A. Riotto, *Phys. Rev. Lett.* **81**, 4048 (1998).
- 49) E. W. Kolb, D. J. H. Chung, A. Riotto, *Phys. Rev. D* **59**, 023501 (1999).
- 50) V. A. Kuzmin, I. I. Tkachev, *JETP Lett.* **68** (1998) 271-275.
- 51) V. A. Kuzmin and V. A. Rubakov, *Phys. Atom. Nucl.* **61**, 1028 (1998).
- 52) M. Birkel and S. Sarkar, *Astrop. Phys.* , **9**, 297 (1998).

- 53) V. K. Dubrovich, D. Fargion, M. Khlopov, *Astropart. Phys.* **22**, 183 (2004).
- 54) V. Berezhinsky, M. Kachelriess, *Phys. Rev. D* **63**, 034007 (2001).
- 55) S. Sarkar, R. Toldra, *Nucl. Phys. B* **621**, 495 (2002).
- 56) C. Barbot, M. Drees, *Phys. Lett. B* **533**, 107 (2002).
- 57) R. Aloisio, V. Berezhinsky, M. Kachelriess, *Phys. Rev. D* **69**, 094023 (2004).
- 58) D. A. Kirzhnits. *JETP Lett.* **15**, 745 (1975).
- 59) V. Berezhinsky, P. Blasi, A. Vilenkin, *Phys. Rev. D* **58**, 103515 (1998).
- 60) V. Berezhinsky, X. Martin, A. Vilenkin, *Phys. Rev. D* **56**, 2024 (1997).
- 61) V. Berezhinsky, A. Vilenkin, *Phys. Rev. Lett.* **79**, 5202 (1997).
- 62) J. J. Blanco-Pillado and K. Olum, arXiv:0707.3460
- 63) T. D. Lee and C. N. Yang, *Phys. Rev.* **104**, 254 (1956).
- 64) L. D. Landau, *JETP* **32**, 405 (1957).
- 65) A. Salam, *Nuovo Cimento* **5**, 299 (1957).
- 66) I. Yu. Kobzarev, L. B. Okun, and I. Ya. Pomeranchuk, *Sov. J. Nucl. Phys.* **3**, 837 (1966).
- 67) L.B. Okun, hep-ph/0606202
- 68) Z. Berezhiani, R. N. Mohapatra, *Phys.Rev. D* **52**, 6611 (1995).
- 69) R. Foot, R. R. Volkas, *Phys.Rev. D* **52**, 6595 (1995).
- 70) V. Berezhinsky and A. Vilenkin, *Phys. Rev. D* **62**, 083512 (2000).
- 71) V. Berezhinsky, M. Narayan, F. Vissani, *Nucl.Phys. B* **658**, 254 (2003).